Fabrication and Test of the LDX Levitation Coil

Philip C. Michael, Alexander Zhukovsky, Bradford A. Smith, Joel H. Schultz, Alexi Radovinsky, Joseph V. Minervini, K. Peter Hwang, and Gregory J. Naumovich

***Abstract*—The Levitated Dipole Experiment (LDX) was designed by Columbia University and the Massachusetts Institute of Technology to investigate plasma confinement within a dipole magnetic field. The experiment consists of a 5 m diameter by 3 m tall vacuum chamber and three superconductor coils: a Nb_3Sn Floating Coil that provides the dipole field for plasma confinement; a NbTi Charging Coil that inductively charges and discharges the Floating Coil current; and a high temperature superconductor (Bi-2223) Levitation Coil that electromagnetically supports the weight of the 620 kg Floating Coil and controls its vertical position within the vacuum chamber.**

LDX is the first U.S. plasma confinement experiment to use a high temperature superconductor coil. The use of high temperature superconductor minimizes the electrical and cooling power needed for levitation, allowing additional power for plasma heating. The levitation coil is a 2800 turn, 1.3 m outer diameter, double pancake winding. It is designed to operate at up to 150 A current at 20 K and is cooled by a combination of one stage cryocooler and liquid nitrogen cooled radiation shield. This paper provides details for the design, fabrication and test of the coil.

***Index Terms*—High temperature superconductor, fusion magnets, conduction cooled superconductor.**

I. Introduction

THE Levitated Dipole Experiment (LDX) is an Innovative Concept fusion experiment that was developed to investigate steady-state, high-beta plasma operation, with near-classical magnetic confinement. Major factors that set LDX apart from earlier experiments are the absence of toroidal field coils, and its emphasis on magnetic flux expansion [1]. Plasma is confined by a single superconductor coil, the Floating Coil (F-coil) [2] that is magnetically supported near the center of a 5 m diameter by 3 m tall vacuum chamber.

The base configuration of the experiment uses a conduction-cooled, disk-shaped, high temperature superconductor Levitation Coil (L-coil), mounted on top of the vacuum vessel, to support the F-coil. For this configuration, the F-coil is stable to tilt and horizontal displacements, thus reducing control requirements for off-axis motions.

The vertical position of the F-coil is sensed optically, and controlled within a ± 1 cm band near the midplane of the vacuum vessel by varying the voltage applied to the L-coil. Feedback control simulations for F-coil positioning anticipate a nominal L-coil operating current of 105 A with a superposed ± 1 A, 1 Hz control current ripple [3]. The largest predicted heat load on the L-coil is magnetization hysteresis loss produced in the HTS conductor by the control current ripple [4]. The predicted a.c. loss is roughly 10 W, assuming full penetration of both the axial and radial field variations into the conductor. To provide margin for larger than anticipated control current ripple and resulting a.c. loss, the L-coil's heat removal path was conservatively designed for an average heat load of 20 W, with a temperature difference between L-coil hot spot and one-stage cryocooler below 2 K.

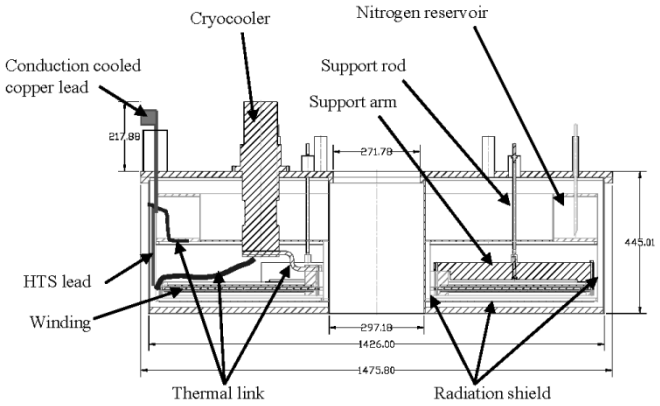

Fig. 1. Section view of the L-coil winding and cryostat.

II. L-Coil Winding and Cryostat

Fig. 1 shows a cross-section view of the L-coil winding and cryostat. The L-coil was fabricated at Everson Electric Company to an MIT design. The L-coil contains approximately 7300 m of American Superconductor Corporation's (ASC) Three-ply Narrow Bi-2223 superconductor. The conductor consists of PIT-processed Bi-2223 in a silver alloy matrix that is clad on both sides with 35 μm stainless steel [5]. Eighteen spools of 440 m conductor length were procured for L-coil fabrication. The average conductor thickness and height were 0.234 mm and 3.0 mm. Each spool contained from zero to three conductor splices per spool, with guaranteed resistance in the superconducting state of less than 200 nΩ per splice. The average self-field critical current for the conductor was 63 A at 77 K.

The main parameters for the L-coil are listed in Table I. The L-coil is a disk-shaped, double pancake winding, with the pancakes wound to either side of a center support plate. The support plate consists of two 1.0 mm (0.04″) thick copper sheets that are epoxy laminated to either side a 9.5 mm (3/8″) thick stainless steel plate. The copper sheets conduct heat from the L-coil to a thick copper ring mounted at the inner diameter of

Manuscript received August 6, 2002. This work was supported by the U.S. Department of Energy under Contract DE-FG02-98ER82529 and Contract DE-FG02-98ER54458.

P. C. Michael, A. Zhukovsky, B. A. Smith, J. H. Schultz, A. Radovinsky, and J. V. Minervini are with the MIT Plasma Science & Fusion Center, Cambridge, MA 02139 USA (e-mail: michael@psfc.mit.edu).

K. P. Hwang and G. J. Naumovich are with Everson Electric Company, Bethlehem, PA 18017 USA (e-mail: phwang@eversonelec.com; gnaumovich@eversonelec.com).

Digital Object Identifier 10.1109/TASC.2003.812808

TABLE I
L-COIL DESIGN PARAMETERS.

Construction	One-in-hand double pancake
Conductor type	ASC Three-ply Narrow conductor
Winding inner diameter	0.41 m
Winding outer diameter	1.32 m
Turns	2 pancakes x 1400 turns each
Total conductor length	7300 m
Turn insulation	76 μm Nomex type N196 tape
Ground insulation	1 layer, 125 μm Nomex N196 sheet
Coil inductance	6.6 H
Operating temperature	20 K
Coil cooling source	Cryomech AL230 cryocooler
Center plate construction	9.5 mm thick stainless steel plate with 1.0 mm thick copper sheets laminated on each side
Center plate inner diameter	0.36 m
Center plate outer diameter	1.36 m
Nominal operating current	~105A, ~65% of coil critical current
Dump voltage	280 V
Weight	~ 180 kg

the coil. This ring is connected through a flexible thermal link to the cryocooler. The stainless steel plate minimizes L-coil deflection when it electromagnetically supports the roughly 620 kg F-coil. The copper sheets are radially segmented to limit eddy current losses and are separated from the stainless steel by 0.25 mm thick glass fabric.

The pancakes are joined at their inner diameters by a 0.51 mm thick by 102 mm long OFHC copper sheet. We fabricated the center transition joint by soldering the ends of two, approximately 1 m lengths of HTS tape near the top and bottom edges of the copper sheet. The assembled joint was insulated, passed through a circumferential slot in the support plate, and loosely shimmed to the proper radial location to begin the winding. Two Teflon®-coated, stainless steel rings with 3.35 mm height and 7.95 mm radial build were bolted to either side of the support plate to provide winding mandrels for the pancakes. The joint lead on the lower side of the support plate was secured and the plate was mounted to the winding turntable. The joint lead on the upper side of the support plate was spliced to the first spool of conductor with indium solder.

Because it was impractical to confirm in-process, the resistance of the superconductor splices made during winding, considerable effort was devoted to the development and qualification of splice fabrication methods. Analysis prior to winding showed that if the splices were free from voids, the splice resistance would be dominated by the conductor's stainless steel cladding [6]. Visual inspection of the soldered joints was considered sufficient to guarantee splice quality. The L-coil contains a total of 34 ASC qualified splices, and 22 splices made during winding.

The L-coil was tension wound using a strain gauge instrumented idler arm and an electrically controlled drag motor, following the winding tension schedule shown in Table II. The tensioning schedule was developed to minimize the accumulation of compressive hoop stresses near the inner diameter of the winding. Each pancake was terminated by indium soldering a 0.51 mm thick by 102 mm long by 12.7 mm tall OFHC copper sheet to the final conductor turn. Five layers of turn insulation were wrapped around the outer diameter of the pancake to complete the ground insulation, followed by ten layers of scrap conductor, to mechanically protect the coil o.d. during subsequent processing.

TABLE II
L-COIL WINDING TENSION SCHEDULE.

Turn numbers	Conductor tension
1 ~ 20	29.0 ± 0.4 N (6.5 ± 0.1 lb)
21 ~ 40	22.3 ± 0.4 N (5.0 ± 0.1 lb)
41 ~ 60	18.3 ± 0.4 N (4.1 ± 0.1 lb)
61 ~ 80	15.6 ± 0.4 N (3.5 ± 0.1 lb)
81 ~ 105	13.4 ± 0.4 N (3.0 ± 0.1 lb)
106 ~ 145	11.1 ± 0.4 N (2.5 ± 0.1 lb)
146 ~ 205	8.9 ± 0.4 N (2.0 ± 0.1 lb)
206 ~ 310	6.7 ± 0.4 N (1.5 ± 0.1 lb)
311 ~ 570	4.5 ± 0.4 N (1.0 ± 0.1 lb)
570 ~ 1400	2.2 ± 0.4 N (0.5 ± 0.1 lb)

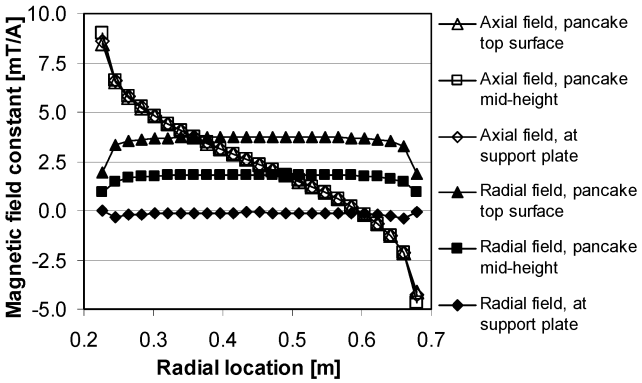

Fig. 2. Variation in the axial and radial magnetic field constants vs. radial location, at three vertical heights in the L-coil upper pancake.

Once the first pancake was complete, it was covered with a layer of ground insulation, an Armalon® parting sheet, and a close fitting potting lid. The coil assembly was flipped over and remounted to the winding turntable to wind the second pancake. After both pancakes were complete, they were epoxy potted to enhance thermal conduction to the support plate copper sheets.

III. ANTICIPATED D.C. PERFORMANCE

The L-coil is optimized to produce the radial field needed for F-coil levitation using minimal conductor volume [4]. The resulting coil design approximates a circumferential directed current sheet and produces a rather unique magnetic field distribution on the L-coil conductor. Fig. 2 plots as a function of radial location, axial and radial magnetic field constants at three axial heights within the upper pancake. The field constants were calculated assuming uniform conductor current density. The radial field constants vary over the single- conductor height of the pancake from near zero at the center support plate to a maximum value of about 3.7 mT/A at its upper surface. At each height in the coil, the radial field is near constant across the coil's radial build. The axial magnetic field constants are uniform over the height of each pancake, but vary from a maximum value of about 8.8 mT/A at the inner diameter to -4.5 mT/A at the outer diameter.

The critical current density of HTS tapes depends on both the magnetic field orientation and the magnetic field intensity. ASC

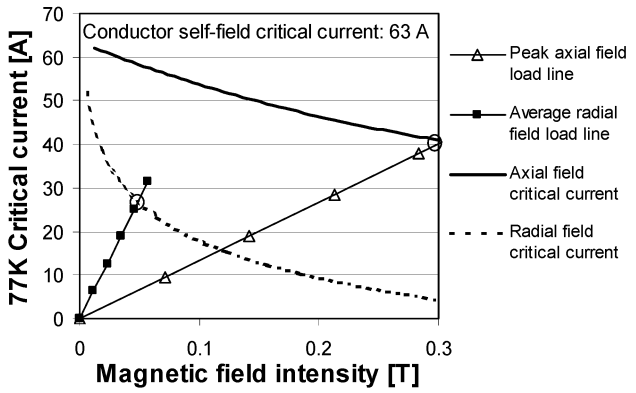

Fig. 3. 77 K critical current vs. background field intensity for L-coil conductor exposed to axial and radial magnetic fields. Load lines for the coil's peak axial field and the average radial field at the mid-height of the pancakes are over-plotted in the figure. The L-coil critical current (28 A) is determined by the lower intersection of load line and critical current curves.

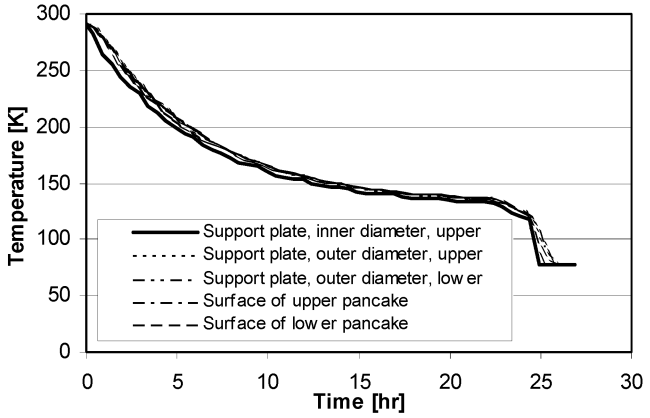

Fig. 4. Temperature vs. time traces during conduction cooling of the L-coil.

provides scaling data that enables their customers to estimate critical currents for various applications based on a conductor's measured 77 K self-field critical current, the background field orientation and intensity, and the operating temperature [7]. Fig. 3 shows the expected 77 K critical current vs. field intensity for the L-coil conductor in both axial and radial field orientations. Representative load lines, for the peak axial field in the pancakes, and average radial field at the pancake mid-height are also plotted in this figure. The intersection of each load line and critical current curve shows the coil's critical current for that field orientation. Fig. 3 indicates that the L-coil critical current is determined by the coil's radial field component. Because the radial field at each height is nearly constant across the coil's radial build, nearly all of the coil should simultaneously exit the superconducting state during a ramped current experiment. The expected L-coil critical current at 77 K is roughly 28 A.

IV. Levitation Coil Test

The L-coil was immersed in liquid nitrogen and tested at 77 K to confirm its viability prior to further integration into the L-coil cryostat. Tests were performed to determine total splice resistance, coil critical current, and normalized a.c. losses.

A. Instrumentation

Voltage taps were installed across each pancake and across the entire L-coil. Five Cryogenic Linear Temperature Sensors (CLTS) were installed to monitor the coil and support plate cool-down temperature profiles. The mounting location included: one sensor each on the top and bottom surfaces of the pancakes at radial locations 0.52 m from the winding axis; and three sensors on the support plate copper sheets, one at the inner diameter of the coil and one each on the top and bottom surface of the support plate at its outer diameter. Two sets of axially directed Hall probes were installed on the top and bottom surfaces of the pancakes at radial locations 0.21 m from the winding axis.

B. Conduction Cooling

The test cryostat was equipped with an internal 15 l liquid nitrogen reservoir that that was placed in the bore of the L-coil and used to conduction cool the L-coil from room temperature to approximately 120 K. Conduction cooling was used to minimize differential thermal stresses during cool-down. Eighty-four strips of AISI 1100, commercial pure aluminum, with 2.5 cm width, 0.41 mm thickness and 0.3 m length were bolted to the top and bottom surfaces of the coil support plate at its inner diameter. The strips were bent up, and over the rim of the reservoir and immersed in liquid nitrogen to begin coil cooling. The height of liquid in the reservoir was controlled with an automated refill system.

Fig. 4 shows the cool-down temperature vs. time traces at various coil locations. All temperatures remained within 20 K of each other throughout cool-down. The cooling rate of the coil was initially about 25 K/hr, but decreased exponentially as the temperature difference between the coil and nitrogen reservoir decreased. As the temperature traces asymptotically approached 130 K, we increased the refill rate for the nitrogen reservoir, and temporarily restored the cooling rate to about 10 K/hr. The rapid cooling observed following 25 hr in Fig. 4 was obtained by filling the test cryostat with liquid nitrogen.

C. DC Performance

The L-coil was connected in series with a 0.3 Ω resistor and energized at several dc voltages between 3 V and -3 V to perform splice resistance measurements. At each series voltage, the coil voltage was recorded after the coil current had settled to a quasisteady value. The total L-coil resistance determined by this method was $12 \pm 3\ \mu\Omega$; this confirms an average resistance of 215 ± 50 nΩ for all conductor splices.

Fig. 5 shows a critical current measurement for the L-coil at a current ramp rate of 0.04 A/s to 38 A current. The inductive voltage in this figure was offset to zero at the start of the current ramp to highlight the critical state transition. The critical current for the L-coil was calculated using the relation:

$$V_{\rm op} = E_c \left(\frac{I_{\rm op}}{I_c} \right)^n l$$

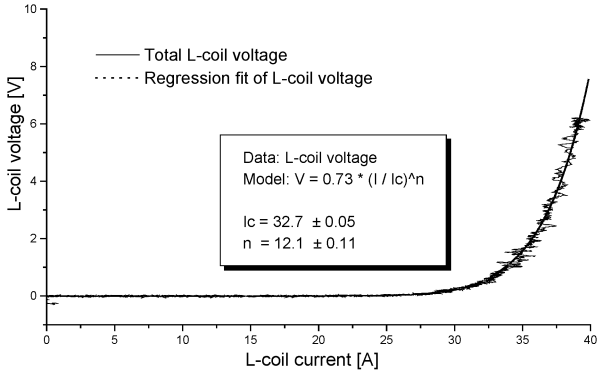

Fig. 5. L-coil voltage vs. current trace during a critical current measurement using a 0.04 A/s current ramp to 38 A.

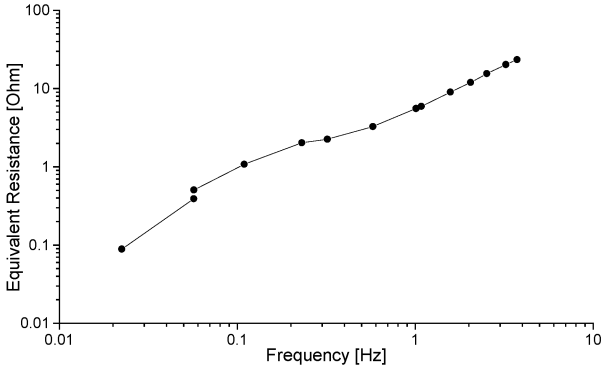

Fig. 6. Equivalent a.c. loss resistance for the L-coil vs. excitation frequency.

where $V_{\rm op}$ is the coil voltage at operating current, $I_{\rm op}$, E_c is the electric field criterion (1 μV/cm) used to define the conductor critical current, n is an "index" number that defines how steep is the critical state transition, and l is the total length of conductor (7300 m) in the L-coil. At 77 K, the measured L-coil critical current was approximately 33 A, with an index number in the range 12–12.2. Both pancakes showed nearly identical critical current values. The measured critical current was roughly 18% larger than the value predicted in Fig. 3.

D. AC Loss

AC losses were measured electronically over the frequency range 0.02 Hz to 4.0 Hz. To perform the measurements, a sinusoidal function generator was connected to 4-quadrant, $\pm$20 V by $\pm$10 A KEPCO power supply, which was used to drive the L-coil. The current amplitude was adjusted at each frequency to remain within the power supply voltage limits. Because a different excitation current was used for each experiment, we first processed the ac loss data by dividing the in-phase voltage component by the coil current to obtain the equivalent loss resistance values shown in Fig. 6. The roughly linear variation of the equivalent loss resistance with frequency is indicative of a hysteresis loss mechanism.

We further processed the loss data to obtain normalized a.c. coil loss energies of 2 to 5 J/cycle at 1 A current excitation; these loss energies are slightly less than, but consistent with our design expectations [4].

V. Conclusion

A high temperature superconductor Levitation Coil was fabricated for the LDX program at Everson Electric Company using ASC conductor. Recent tests with the L-coil immersed in liquid nitrogen confirm the coil performance with respect to its design predictions. The L-coil cryostat is under fabrication at Everson Electric and system integration should be complete by the end of the year.

Acknowledgment

The authors thank the American Superconductor Corporation for its leadership in the U.S. Department of Energy, Office of Fusion Energy Sciences Phase II SBIR program that supported the L-coil construction. They especially thank L. Masur and A. Otto, whose efforts were vital to the project.

References

[1] J. Kesner, L. Bromberg, D. Garnier, and M. Mauel, "Plasma confinement in a magnetic dipole," in *Fusion Energy 1998*, vol. 3. Vienna, 1999, p. 1165.

[2] B. A. Smith *et al.*, "Design, fabrication and test of the react and wind, Nb_3Sn, LDX floating coil," *IEEE Trans. Appl. Superconductivity*, vol. 11, pp. 2010–2013, Mar. 2001.

[3] T. S. Pederson *et al.*, "Computer simulations and design of levitation feedback control system for the levitated dipole experiment," presented at the 42nd Annual Meeting of the APS Division of Plasma Physics with the 10th International Congress on Plasma Physics, Quebec City, Canada, Oct. 2000. presented.

[4] J. H. Schultz *et al.*, "High temperature superconducting levitation coil for the levitated dipole experiment (LDX)," *IEEE Trans. Appl. Superconductivity*, vol. 11, pp. 2004–2007, Mar. 2001.

[5] L. Masur *et al.*, "Long length manufacturing of BSSCO-2223 wire for motor and cable applications," *Adv. Cryo. Eng.*, vol. 46, pp. 871–877, 2000.

[6] P. Michael, "Joint Resistance Estimates for L-Coil Splices, Rev. 1," MIT, Cambridge, MA, LDX Project Memo LDX-MIT-PMichael-083 001-01, Aug. 30, 2001.

[7] *Bi-2223 High Strength Reinforced Wire Fact Sheet*.